

# Autonomous Science Target Touchability Evaluation: A Fuzzy Logic-Based Approach

Chen Gui and Changjing Shang<sup>(✉)</sup>

Department of Computer Science, Institute of Mathematics,  
Physics and Computer Science, Aberystwyth University,  
Aberystwyth SY23 3DB, UK  
{chg12,cns}@aber.ac.uk

**Abstract.** Currently, for Mars science target selection, the task of determining whether or not it is possible for a robot arm to touch a target is accomplished by human operators and scientists on Earth. The development of useful on-board autonomous touchability techniques would greatly reduce human intervention. It would be advantageous if the rover could evaluate autonomously whether the robot arm would be able to place an instrument against an identified science target. In this paper we propose a new approach to the problem of autonomous science target touchability evaluation. We assess the touchability of a potential science target in terms of its size (the number of pixels of the science target in the image), SV (the science value of the science target), distance (the reachable distance of a robot arm), and orientation (the angular regions of the arm's shoulder azimuth). In particular, the plane in front of the arm is divided into a number of partitions, which are ranked with the different touchability levels by the use of a fuzzy rule-based system. Simulations on the rank of science object touchability are carried out, via software and hardware implementation. Based on the real data gathered from the cameras and the Schunk arm experimental results successfully verify the validity of the proposed approach.

**Keywords:** Fuzzy logic · Target touchability · Autonomous evaluation

## 1 Introduction

Owing to the high cost and risk of manned space exploration missions, space agencies primarily concentrate on unmanned planetary exploration. The most advanced exploration robots that have been deployed for planetary exploration are the Mars Exploration Rover (MER, “Spirit” and “Opportunity”) and the Mars Science Laboratory (MSL, “Curiosity”). They both have an identical manipulation scenario, consisting of four main stages for science target exploration: (a) The rover on Mars transmits the images captured from the navigation camera to the operators/scientists on Earth, with an interesting target being manually selected by the ground scientists in a stereo range map. (b) A target tracker enables the rover to autonomously drive to its goal position while

avoiding obstacles, and to reach the goal position with the precision of a few centimetres. (c) The scientists artificially designate the sampling point on the scientific goal from the downlinked images. (d) A variety of instruments on-board are utilised in order to sample and analyse the science target.

In order to determine whether a science goal can be acquired, both MER and MSL adopt a rigid approach using the robot arm workspace. For instance, in terms of the Curiosity rover the workspace volume is an upright cylinder 80cm diameter, 100cm high, positioned 105cm in front of the rover when it is on a smooth flat terrain [1]. Therefore, the current mechanical strategy employed by MER and MSL is that the science target is deemed to be able to be acquired just when it is within the robot arm workspace. This strategy does not consider the cases where an interesting target is surrounded by other rocks that can not be traversed in the ‘*rock garden*’, which is not able to get into the robot arm workspace but is just on the edge of the workspace. This problem can be addressed if the robot arm workspace is variable based on the distinct characteristic of a given target. We propose an autonomous flexible approach to adjusting automatically the robot arm workspace in relation to the science value score (SV) regarding the scientific goal. This strategy is based on the use of fuzzy logic techniques, capable of increasing appropriately the magnitude of the robot arm workspace when the science value score is high.

Our work is inspired by the observation that the application of fuzzy logic in planetary exploration has recently gained significant recognition. Traditionally, the difficulty level a rover may encounter when attempting to traverse a region of terrain in a no priori knowledge environment, is classified through the use of traversability index [2]. Howard et al. [3] extended this approach by combining it with a fuzzy map representation that reflects the traversal difficulty of the terrain. It concentrates on planning over an optimally safe path of minimum traversal cost. Mahmoud [4] utilised a fuzzy adaptation technique that examines the population of paths throughout the execution of the underlying algorithm while adjusting operator probabilities to attain better solutions for path planning. Fuzzy logic has also seen applied to planetary landing and the tier-scalable robotic planetary reconnaissance. For example, in addressing the issue of landing site selection [5], the score of each potential candidate landing site is obtained from sensor measurements that are fed into a fuzzy system which decides on spatial and temporal dependence. Furfaro et al. [6] built a fuzzy system where the appropriate past/present water/energy indicators can be acquired when the tier-scalable mission framework is deployed, and used to estimate the habitability on Mars. Also, in dealing with the first-stage of the aforementioned operational scenario, Barnes et al. [7] and Pugh et al. [8], proposed that a fuzzy rule based expert system (KSTIS 1.0) could be used. Such a system adopts knowledge elicitation from a planetary geologist to obtain the primary clues regarding the geological background (*Structure, Texture and Composition*) of Martian rocks, and generates a useful science value score (SV) with respect to each rock in an image.

The rest of this paper is organised as follows. A brief overview of the proposed touchability system framework is presented in Section 2, with a focus

on the construction of the linguistic fuzzy sets and the fuzzy rules associated with the underlying attributes that are utilised by the system. Results of computer simulation are reported in Section 3, as part of the verification of the proposed approach. Further experimental results though hardware implementation are described in Section 4, comparing the proposed approach against the performance attainable by a domain expert. The paper is concluded in Section 5.

## 2 Proposed Touchability System

The structure of the proposed fuzzy logic-based touchability system is shown in Figure 1. It consists of six main components: a vision system, the Knowledge based Science Target Identification System (KSTIS 1.0), a fuzzification module, a fuzzy inference engine, a rule base and a defuzzification module. In this system the input data  $i_d, i_o, i_s$  are: the distance between the robot arm base and the centroid of a possible science target, the orientation of the arm's shoulder azimuth, and the size of the target in the image, respectively. The output  $o_t$  from the proposed fuzzy system is the touchability probability for each identified scientific target. KSTIS 1.0 assists in ground-based interpretation of scientific targets [7,8], from the description of the *Structure*, *Texture* and *Composition* of a scientific target whose values are provided by scientists/experts on Earth, giving the score of *Science Value*  $i_{SV}$ .

The proposed approach is easy to comprehend and is simple to implement. It basically adopts the general structure of a conventional fuzzy logic controller, with the functionalities of its key components described below. Note that although simplistic in implementation, the underlying techniques adopted are well formed with solid mathematical foundations that have been developed in the field of fuzzy logic control. This forms a sharp contrast with typical existing mechanisms to assess the touchability that are largely based on use of ad hoc methods.

**Fuzzification.** This module maps the crisp input values onto their corresponding linguistic fuzzy terms. This involves the four physical properties indicated previously: Size, Distance, Orientation and SV of a possible target.

*Size ( $i_s$ ):* The bounding area of a given object within an image is characterised as the size of the object. One way to identify the surroundings of an object such as that used by MER is to form a detailed DEM (Digital Elevation Model) by accomplishing stereo matching over the full images. However, in order to obtain just the essential information on size efficiently, only 5 points per object are herein applied for stereo matching as shown in Figure 2. The minimum rectangle ( $A, B, C$  and  $D$ ) for each edge inscribes the leftmost, rightmost, uppermost and bottommost points (P3, P4, P1 and P2) of the object, respectively, while  $E, F, G$  and  $H$  are the middle points of the line segments 'AB', 'BC', 'CD' and 'AD', respectively. The point C0 is the cross point of the line segments 'EG' and 'HF' and is the centroid of the object. P1, P2, P3 and P4 represent the stereo

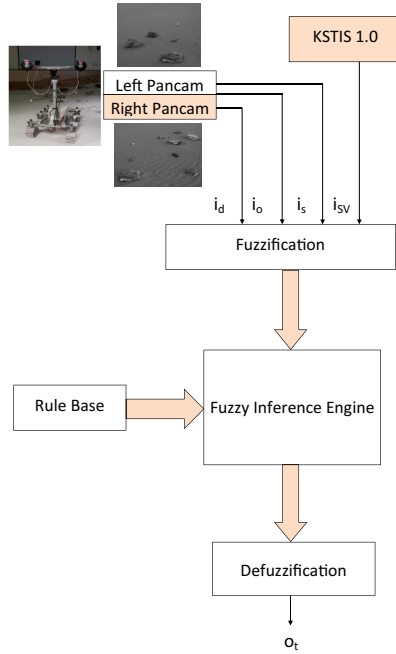


**Fig. 1.** Fuzzy logic touchability evaluation system.

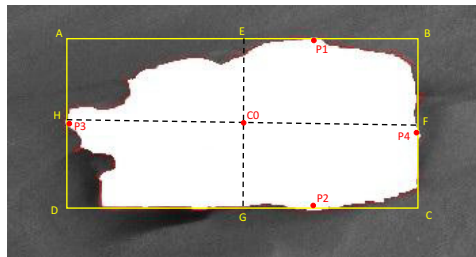


**Fig. 2.** Stereo matching points selection.

matching points, whose three dimensional frame values are then derived by the external and internal parameters of the cameras. The membership functions of these fuzzy sets are empirically defined as given in Figure 3.

*Distance ( $i_d$ ):* This is a significant variable in this study, whose span is provided by the length of the robot arm. Figure 4 illustrates the distance between the original point  $O$  in the mobile robot arm base and the centroid ( $C$ ) of an object. The membership functions of the relevant fuzzy sets are given in Figure 5.

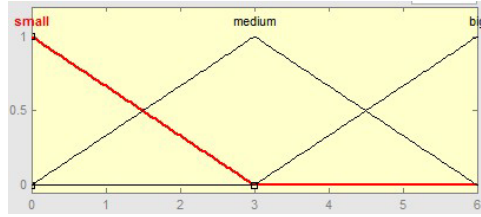


**Fig. 3.** Membership functions for Size ( $i_s$ ).

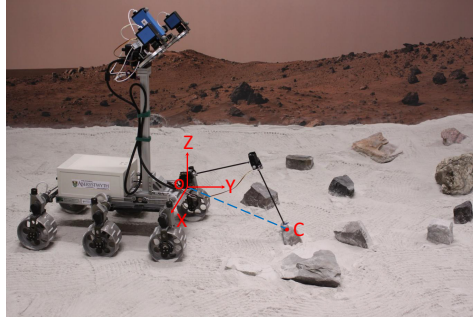


**Fig. 4.** Distance between arm and object.

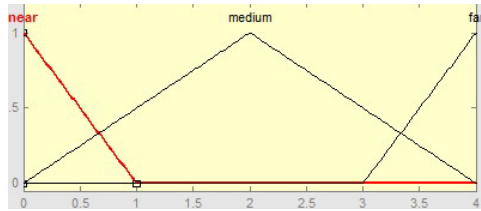


**Fig. 5.** Membership functions for Distance ( $i_d$ ).

*Orientation ( $i_o$ ):* This is the angle formed by the straight line defined relative to the heading of the rover, and the straight line that connects the projection of the centroid of the object with the reference arm, as shown in Figure 6. As highlighted in the figure,  $C'$  is the projection of  $C$  on the plane that is constituted by the  $X$  and  $Y$  axes.  $\theta$  is an angle between the straight line  $OC'$  and  $Y$  axis, and is the orientation. In Figure 7, the orientation in front of the rover is divided into six regions that are represented by six linguistic fuzzy sets  $\{very\text{-}bad(VB), bad(B), very\text{-}soso(VS), soso(S), good(G), very\text{-}good(VG)\}$ . The “very-good”, “good”, “soso”, “very-soso”, “bad” and “very-bad” are sectors at  $\pm 15^\circ$  (Red), between  $\pm 15^\circ$  and  $\pm 30^\circ$  (Turquoise), between  $\pm 30^\circ$  and  $\pm 45^\circ$  (Yellow), between  $\pm 45^\circ$  and  $\pm 60^\circ$  (Green), between  $\pm 60^\circ$  and  $\pm 75^\circ$  (Orange), and between  $\pm 75^\circ$  and  $\pm 90^\circ$  (Pink) relative to the heading of the

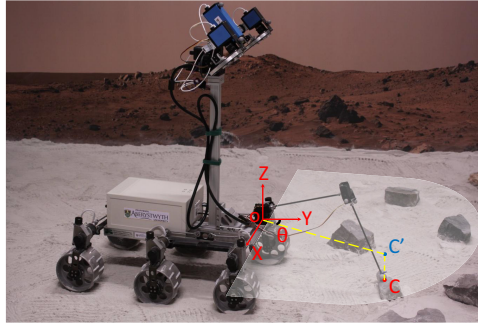


Fig. 6. Orientation between arm and object.

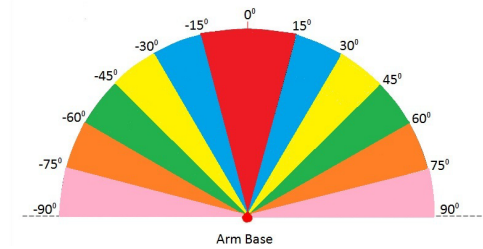


Fig. 7. Decomposition of orientation regions.

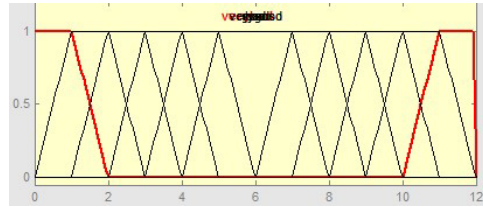
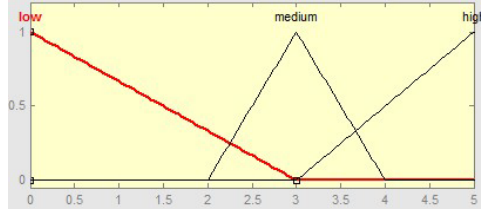


Fig. 8. Membership functions for Orientation ( $i_o$ ).

rover, respectively. The membership functions of these sets are shown in Figure 8 in which “0”, “2”, “4”, “6”, “8”, “10” and “12” are corresponding to  $-90^\circ$ ,  $-60^\circ$ ,  $-30^\circ$ ,  $0^\circ$ ,  $30^\circ$ ,  $60^\circ$  and  $90^\circ$ , respectively.

*Science Value (SV) ( $i_{SV}$ ):* This is a score between 0 and 9999, computed by KSTIS 1.0. It is represented by one of the three linguistic fuzzy sets {LOW, MEDIUM, HIGH}, with the corresponding membership functions defined as given in Figure 9.

Note that as illustrated above, all fuzzy sets used in this system are implemented with triangular membership functions. This is mainly due to the relative simpler computation this type of fuzzy set entails as compared to the use of typical alternatives such as trapezoidal or Gaussian functions. The employment of



**Fig. 9.** Membership functions for SV ( $i_{SV}$ ).

triangular membership functions is also partially because of the relative ease in communicating the underlying mathematical concepts between the knowledge engineers and domain experts.

**Inference Mechanism.** This is responsible for decision-making in the fuzzy system through fuzzy reasoning. It achieves two tasks: (1) to determine the extent to which each rule in the rule base is associated with the current situation as characterised by the inputs; and (2) to derive a conclusion by firing the best matching rule. Seventy-four rules are included in the rule base, including the 72 general rules shown in Figure 10 and the following two specific ones (that human experts believe to be of significance for the present investigation):

- IF Size is SMALL THEN TIndex is VERYLOW
- IF SV is LOW THEN TIndex is VERYLOW

**Defuzzification.** The output of the fuzzy inference mechanism is mapped onto a crisp value, called *Touchability Index* by this module. There are a number of methods that can be used to implement this inverse operation of fuzzification. The “COG defuzzification” is herein used to combine the outputs represented by the implied fuzzy sets from all rules that at least partially match the inputs to form a single overall output. The *Touchability Index* is represented by seven fuzzy sets {VERYLOW, LOW, MEDIUMLOW, MEDIUM, MEDIUMHIGH, HIGH, VERYHIGH}, whose membership functions are shown in Figure 11.

### 3 Software Simulation

This section presents experimental results of computer-based simulation, comparing the resulting *Touchability Index* of mock objects in terms of their ranks with that given by a human expert. The system is implemented using MATLAB Fuzzy ToolBox simulator and involves 9 artificially created rock objects, of three different types: small ( $10 \times 15$ ), medium ( $20 \times 15$ ) and big ( $30 \times 20$ ). Here, the length of the Curiosity rover arm has been employed for simulation experiments, which is 2.3 meters from the front of the rover body. The three science value scores used are 35, 65 and 105. In Table 1,  $Length \times Width$  is the size of an object.

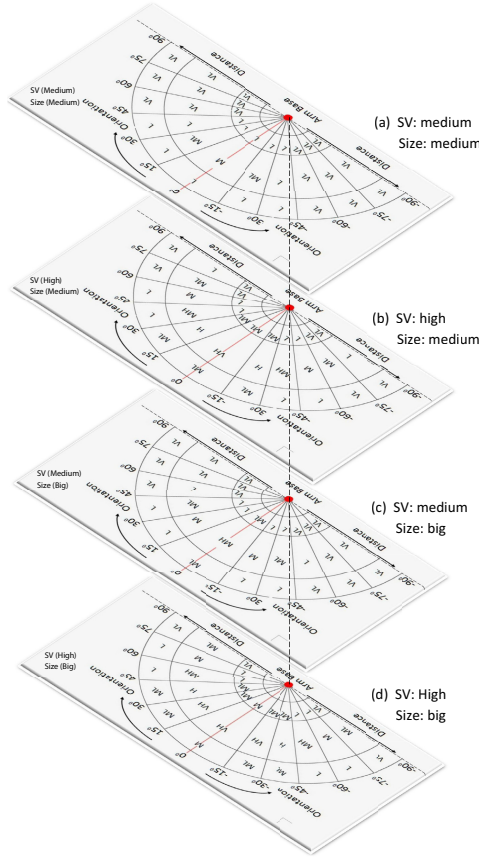


**Fig. 10.** Rule base for touchability (VL-VeryLow, L-Low, ML-MediumLow, M-Medium, MH-MediumHigh, H-High, VH-VeryHigh).

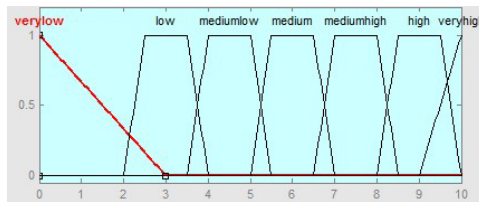


**Fig. 11.** Membership functions for Touchability Index ( $o_t$ ).

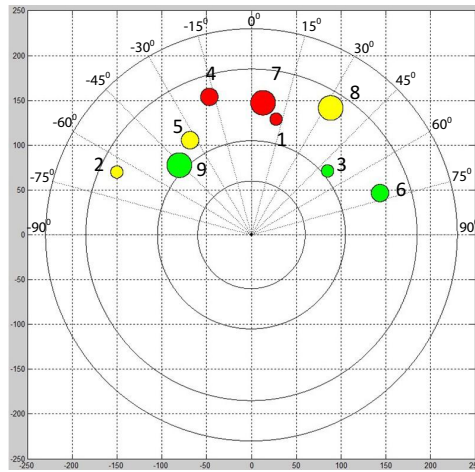
Figure 12 shows the resulting rock ranking. The centre of the frame is the arm base, the SV is represented by colour, with the relevant colour coding defined in Table 2, and the size of the rock is depicted by the diameter of the colour circle. It summarises that the touchability sequence of these rocks can be intu-










**Table 1.** Experimental data for simulation.

Rock No.	Length	Width	SV	Orientation	Distance
1	10	15	105	12	132
2	10	15	65	-65	166
3	10	15	35	50	111
4	20	15	105	-17	161
5	20	15	65	-33	126
6	20	15	35	72	151
7	30	20	105	5	148
8	30	20	65	32	167
9	30	20	35	-46	112

itively ranked as shown in Table 3, where the rank is sorted with respect to the magnitude order of the *Touchability Index*, *TIndex*. These results compare perfectly with those given by the human expert, demonstrating the validity of the proposed approach.

**Fig. 12.** Simulated experiment environment.**Table 2.** Correspondence between SV and colour.

Corresponding Colour							
SV Score	<20	20-39	40-59	60-79	80-99	100-119	>120

**Table 3.** Simulation-based experimental result.

RockNO.	Human Rank	TIndex(%)	TRank
1	5	35.2	5
2	7	23.8	7
3	8	22.3	8
4	2	88.4	2
5	4	54.1	4
6	9	18.4	9
7	1	96.6	1
8	3	67.5	3
9	6	34.9	6

## 4 Hardware Implementation

This section reports results on the use of real rocks and data to further verify the validity of the proposed approach for fuzzy logic-based touchability evaluation through hardware implementation. All images taken are segmented manually, with the measurement method described in [9] used to determine the size of each rock. The evaluation given by the domain expert is used as the ground truth in this study. The experimental hardware platform that is implemented to perform this set of experiments includes a robot arm, two wide-angle cameras (WACs), a camera mast and an optical bench, as shown in Figure 13.

A total of 9 rocks of a different size and shape are used in this experimentation. Within the 9 rocks there are 3 small, 3 medium and 3 big ones, each type of rock involving three different scientific values: Low, Medium and High. The science value of each rock is given by the domain expert. The length of the Schunk arm is 1 meter, and the overlap vision range of the two cameras is approximately between  $-30^\circ$  and  $30^\circ$ . Seven experiments are carried out based on the location of these 9 rocks (Near, Medium and Far). The evaluation from the domain expert for all experiments is that the Touchability Index should be at least 80%.

As all experiments have a conceptually similar set up, to save space, only that for the first experiment is shown here, as given in Figure 14. This experiment involves four target situations: (1) Rock 1 is a big one, and has a high science value; its distance to the robot arm is medium. (2) There is a low scientific value for the small Rock 2 with a medium distance. (3) A high science value and a medium distance are assumed for small Rock 3. (4) Small rock 4 possesses a medium scientific value and is of a near distance to be robot arm. The evaluation of the touchability given by the domain expert for these four rocks is that only Rock 1 is touchable. Figure 14 shows the result produced by the Schunk arm. The Touchability Index and the relevant measurement computed are presented in Table 4.

As specified by the domain expert, a positive result is achieved if the computed Touchability Index over a certain rock is greater than 80%. In this first experiment only the Touchability Index over Rock 1 (92.5%) is greater than

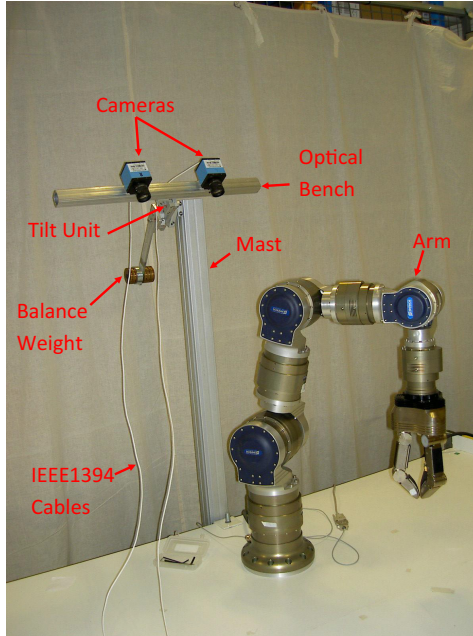


**Fig. 13.** Experimental platform.

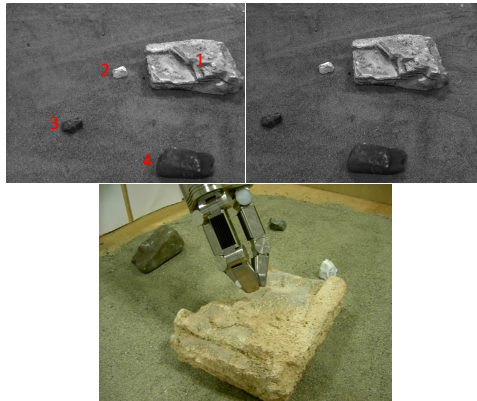


**Fig. 14.** Top left image: captured by the left camera. Top right image: captured by the right camera. Bottom image: result of touchability computation.

80%. This means that the robot arm can reach out for this rock but not the rest. This result matches well with the evaluation of the domain expert. Similar results are obtained for experiments 4 and 6.

In experiment two the Touchability Index over all rocks is less than 80%, so the robot arm cannot reach any rocks. The evaluation of the touchability given

**Table 4.** Results from the first experiment.

Rock No.	Size ( $cm^2$ )	Orientation	Distance ( $cm$ )	Science Value	Touchability Index
1	737.86	18°	76.4	120	92.5%
2	26.33	-6°	75.3	40	9.76%
3	24.4	-25°	52.7	100	9.75%
4	109.46	20°	37.6	90	21.6%

by the domain expert is the same. Similar results are obtained for experiments three, five and seven also, although different rocks and different numbers of rocks are involved in those experiments.

Summarising the above experimental results, it is clear that the evaluation outcomes of using the present approach match fully with those attainable by the domain expert in a range of target settings. This implies that the fuzzy logic-based touchability system designed herein is capable of achieving the experience and knowledge level of the domain expert.

## 5 Conclusions

In this paper, a fuzzy logic-based system for autonomous touchability evaluation of space science targets has been presented. The membership functions and fuzzy rules have been devised and the defuzzification mechanism identified. The approach has been implemented in both software and hardware. Simulation-based experimentation has shown the validity of the proposed system, which has been further confirmed by the results of seven independent experiments on real settings, over different rock locations, sizes and science values. The system has proven to be able to achieve the performance of a domain expert. Whilst successful, further research remains. This includes an investigation of whether the approach is sensitive to the use of different fuzzification and defuzzification methods, and a study of how fuzzy rules may be learned from historical missions.

## References

1. Anderson, R.C., Jandura, L., Okon, A.B.: Collecting Samples in Gale Crater, Mars; an Overview of the Mars Science Laboratory Sample Acquisition, Sample Processing and Handling System. *Space Science Reviews* **170**, 57–75 (2012)
2. Seraji, H.: Traversability index: a new concept for planetary rovers. In: *Proceedings of IEEE International Conference on Robotic and Automation* (1999)
3. Howard, A., Seraji, H., Werger, B.: Fuzzy terrain-based path planning for planetary rovers. In: *Proceedings of IEEE International Conference on Fuzzy Systems*, pp. 316–320 (2002)
4. Mahmoud, T.: Hybrid Intelligent Path Planning for Articulated Rovers in Rough Terrain. *Fuzzy Sets and Systems* **159**, 2927–2937 (2008)

5. Navid, S., Homayoun, S.: Landing site selection using fuzzy rule-based reasoning. In: Proceedings of International Conference on Robotics and Automation, pp. 4899–4904 (2007)
6. Furfaro, R., et al.: The Search for Life Beyond Earth through Fuzzy Expert Systems. *Planetary and Space Science* **56**, 448–472 (2008)
7. Barnes, D., Pugh, S., Tyler, L.: Autonomous science target identification and acquisition (ASTIA) for planetary exploration. In: Proceedings of International Conference on Intelligent Robots and Systems, pp. 3329–3335 (2009)
8. Pugh, S., Barnes, D., Tyler, L.: AUPE-A PanCam emulator for the ExoMars 2018 mission. In: Proceedings of International Symposium on Artificial Intelligence, Robotics and Automation in Space (2012)
9. Gui, C., Barnes, D., Pan, L.: A Method for matching desired non-feature points to size martian rocks based upon SIFT. In: Proceedings of Towards Autonomous Robotic System Conference (2014)